

~~CONFIDENTIAL~~

RM A53BO2

NACA RM A53BO2

6406


 TECH LIBRARY KAFB, NM
 0143581

RESEARCH MEMORANDUM

AN EXPERIMENTAL INVESTIGATION OF THE ZERO-LIFT-DRAG
 CHARACTERISTICS OF SYMMETRICAL BLUNT-TRAILING-EDGE
 AIRFOILS AT MACH NUMBERS FROM 2.7 TO 5.0

By Clarence A. Syvertson and Hermilo R. Gloria

Ames Aeronautical Laboratory
 Moffett Field, Calif.

Classification changed (or changed to) Unclassified
 By Nasa Tech Pub Announcement #98
 (R AUTHORIZED TO CHANGE)

By

26 Mar 56

NK

GRADE OF

7 Apr 61
 DATE

This material contains information affecting the National Defense of the United States within the meaning of the espionage laws, Title 18, U.S.C., Sec. 793 and 794, the transmission or revelation of which in any form to an unauthorized person is prohibited by law.

NATIONAL ADVISORY COMMITTEE FOR AERONAUTICS

WASHINGTON

April 29, 1953

RECEIVED
RECEIVED

319.98/13

~~CONFIDENTIAL~~

~~7-227~~



NATIONAL ADVISORY COMMITTEE FOR AERONAUTICS

RESEARCH MEMORANDUM

AN EXPERIMENTAL INVESTIGATION OF THE ZERO-LIFT-DRAG

CHARACTERISTICS OF SYMMETRICAL BLUNT-TRAILING-EDGE

AIRFOILS AT MACH NUMBERS FROM 2.7 TO 5.0

By Clarence A. Syvertson and Hermilo R. Gloria

SUMMARY

The zero-lift-drag characteristics of nine symmetrical airfoils were investigated experimentally at Mach numbers from 2.7 to 5.0 and Reynolds numbers (based on the chord) from 0.35 million to 3.63 million. Eight of these airfoils had blunt trailing edges and were designed to have minimum pressure drag at a Mach number of 3 or 5 for a given torsional rigidity or a given bending strength. The ninth airfoil was a conventional biconvex section having a torsional rigidity equal to that of three of the minimum-drag airfoils. Section thickness ratios varied from 3.74 to 6.10 percent. It was found that each minimum-drag airfoil had, at its design Mach number, the lowest drag of all airfoils tested having the same structural requirement. The differences in drag of comparable sections were found to be smaller at the higher Mach numbers, apparently because of a decrease in pressure drag relative to skin-friction drag.

Experimentally determined surface pressures compared favorably with the predictions of a high Mach number, small-deflection angle approximation to shock-expansion theory. In this connection it was found necessary to consider distortion of the airfoil profile by the laminar boundary layer at the higher test Mach numbers.

Measured base pressures on the minimum-drag airfoils are presented. These data are found to correlate against a parameter proportional to the ratio of the boundary-layer height at the trailing edge to the base height.

INTRODUCTION

Drougge (ref. 1) was among the first investigators to study airfoil profiles for minimum pressure drag at supersonic speeds. By the use of

linear theory, sections with sharp trailing edges were determined, having minimum pressure drag for given thickness ratio, cross-sectional area, or moment of inertia. Chapman (refs. 2 and 3) pointed out, however, that further reductions in pressure drag (up to 30 percent in some cases) could be obtained by the use of airfoils with blunt trailing edges. In reference 3, general methods for determining blunt-trailing-edge airfoils with minimum pressure drag were formulated and a rather complete group of structural requirements was considered. The methods of analysis were applied to linearized supersonic flow. More recently, blunt-trailing-edge airfoils for minimum pressure drag have been determined using non-linear theories. Klunker and Harder (ref. 4) used the slender-airfoil theory of reference 5, and Chapman (ref. 6) used shock-expansion theory (see, e.g., ref. 7). Inherent to all the analyses of blunt-trailing-edge airfoils is the fact that the base pressure must be known in order to determine an airfoil with minimum pressure drag. Thus far, base pressures have not been predicted accurately by theoretical methods.

At high supersonic airspeeds, these analyses indicate that minimum-pressure-drag sections will have relatively large degrees of bluntness, and furthermore that the savings in pressure drag over more conventional sharp-trailing-edge sections will be relatively large. These theoretical findings emphasize the need for comparable experimental data; however, there seems to be very little available for any of the predicted minimum-drag sections. Particularly is this the case for airfoils designed for a specified structural requirement, such as a given torsional rigidity or a given bending strength. An experimental investigation of the zero-lift-drag characteristics of such airfoils at high supersonic speeds is, therefore, the subject of the present report.

This investigation was undertaken with three aims. The first aim was to check experimentally the accuracy of the airfoil theory used to design the test airfoils. These airfoils were designed using shock-expansion theory after the method of reference 6, since it has been shown (ref. 8) that at high supersonic airspeeds the predictions of this theory compare most favorably with those of the more exact method of characteristics. The second aim was to ascertain at high supersonic Mach numbers the reliability of the method of reference 9 for estimating and correlating the base pressures acting on the test airfoils. This method was employed for the purposes of the present investigation since it has proven relatively reliable at low supersonic speeds. The third aim was to compare experimentally several airfoils of equal structural properties to determine insofar as is possible whether or not the predicted (designed) shapes do indeed have the lowest drag for their particular design conditions. To these ends, nine airfoil sections were tested at Mach numbers from 2.7 to 5.0 and Reynolds numbers (based on the chord) from 0.35 million to 3.63 million.

SYMBOLS

- C_D drag coefficient, $\frac{\text{drag}}{qS}$
- C_p pressure coefficient, $\frac{p_1 - p_o}{q_o}$
- c chord, in.
- h airfoil base height, in.
- M Mach number (ratio of local velocity to local speed of sound)
- p static pressure, lb/sq in.
- q dynamic pressure, lb/sq in.
- Re Reynolds number (based on chord)
- S exposed wing area, sq in.
- t airfoil thickness, in.
- x airfoil abscissa, in.
- y airfoil ordinate, in.

Subscripts

- o free-stream conditions
- b conditions at airfoil base
- 1 conditions on surface

EXPERIMENT

Test Apparatus and Techniques

All tests were conducted in the Ames 10- by 14-inch supersonic wind tunnel, which is of the continuous flow, nonreturn type with a nominal reservoir pressure of six atmospheres. Stream Mach numbers can be varied from 2.7 to 5.0 by changing the relative positions of the symmetrical

nozzle blocks. A more complete description of the wind tunnel and its auxiliary equipment can be found in reference 10.

The wings were tested in combination with a slender body of revolution having a fineness ratio of 14.25. Total-drag forces acting on the wing-body combination at zero lift were measured by a strain-gage-type balance. Measured tare drag acting on the support body was subtracted from the measured total drag to give the net drag on the airfoil.¹ Tare forces on the sting supports for the models were essentially eliminated by shrouding that extended to within 0.06 inch of the support-body base.

Base pressures were measured on the support body and the blunt-trailing-edge airfoils with McLeod type low-pressure manometers. Reservoir pressures were measured with a Bourdon type pressure gage, and static, dynamic, and pitot pressures were determined from tunnel calibration data. Stream Mach numbers were determined from ratios of these static and pitot pressures.

Models

Eight blunt-trailing-edge airfoils, designed by the method of reference 6 to have minimum pressure drag at zero lift for a given structural requirement and a given Mach number, were used in this investigation. The structural requirement was either a given torsional rigidity or a given bending strength. With the method of reference 6, it is necessary to know in advance the variation of base pressure with Reynolds number, Mach number, and airfoil shape (especially base height). An approximation to this variation was obtained by estimating the effect of Mach number on the curves of correlated base-pressure data presented in reference 9 (see discussion of base-pressure data).

Airfoils with torsional rigidity specified.- The first airfoil section was designed to have minimum pressure drag at a Mach number of 3 for a given torsional rigidity (moment of inertia about the chord axis).² Since it was difficult to specify arbitrarily a reasonable numerical value of the moment of inertia, the procedure was to take the value that

¹Interference drag is therefore included in the drag results presented.

In this connection, however, it was observed in reference 11 that the interference drag is small, at least at low supersonic Mach numbers, for wing-body combinations of the type tested if the wings are defined as the exposed half-wings joined together. It might be expected that the interference drag would be even less at the present test Mach numbers.

²The sections were considered to be solid. In the notation of reference 6, this is the case where $n = 3$ and $\sigma = 0$. It also corresponds to a given bending stiffness.

corresponded to the first airfoil section with a thickness ratio of 6 percent. The second airfoil was designed to have minimum pressure drag at a Mach number of 5 for the same torsional rigidity as the first airfoil.

Airfoils with bending strength specified.- The third airfoil section was designed to have minimum-pressure drag at a Mach number of 3 for a given bending strength (section modulus).⁸ Again in this case, it was difficult to specify offhand a reasonable numerical value of the section modulus. The procedure was to adjust the value of the design section modulus until the moment of inertia was equal to that of the first two airfoils. This was done to enable an additional comparison of the two types of minimum-drag airfoils. The fourth airfoil was designed to have minimum drag at a Mach number of 5 for the same bending strength as the third airfoil.

A second family of airfoils was then designed following this same procedure, only the thickness ratio of the first airfoil was 4 percent. Thus, the airfoils fall into two families according to thickness ratio. The airfoils in one family are approximately 6 percent thick; those in the other, approximately 4 percent thick. In each family, then, there are four airfoils; two are designed for a given torsional rigidity and two for a given bending strength. One of each type is designed for a Mach number of 3; the other for a Mach number of 5. Three of the airfoils have the same torsional rigidity; two have the same bending strength. In addition to the eight minimum-drag profiles, a ninth airfoil with a parabolic-arc biconvex section was designed to have the same moment of inertia as the torsional-rigidity airfoils in the thicker (6 percent thick) family. The biconvex airfoil has a sharp trailing edge and is 6.10 percent thick. This airfoil is included to aid in comparing the minimum-drag airfoils to more conventional shapes. The design conditions and the method of identifying each airfoil are given in table I. The coordinates of all the airfoils tested are presented in table II, and a sketch of the different airfoil profiles is presented in figure 1.

All airfoils tested were made of polished steel with a chord of 2 inches and exposed span of 3 inches. A photograph of the airfoils tested is presented in figure 2. The force models were supported in the wind tunnel on an 0.875-inch-diameter body having a minimum-pressure-drag nose (see ref. 10 for optimum body of given fineness ratio) of fineness ratio 7, faired to a cylindrical body of fineness ratio 7.25. A picture of the entire test assembly is shown in figure 3. Each of the blunt-trailing-edge airfoils had four orifices in the base which were used to measure the base pressure. A sketch of a typical airfoil showing the location of the orifices is presented in figure 4.

⁸Again the sections were considered to be solid. In the notation of reference 6, this is the case where $n = 3$ and $\sigma = 1$.

In addition to the force models, a model of airfoil 306-T (designed for $M_0=3$, approximately 6 percent thick, and having a given torsional rigidity; see table I), having a chord of 4 inches and a span of 4 inches, was constructed to measure the chordwise pressure distribution. This model had a single row of orifices along the midspan. Only the side of the airfoil containing the pressure orifices was contoured; the other side of the airfoil was made a simple wedge of relatively larger thickness in order to increase structural strength. A photograph of this model is presented in figure 5.

Accuracy of Results

Surface and base pressures, measured on McLeod type manometers, are accurate to within ± 1 percent of true pressures. At free-stream Mach numbers of 4.48 and above, the measured base pressures were influenced by some condensation of the air. Condensation partially inhibits expansion about the base and thus leads to higher base pressures than would be expected in the absence of this phenomenon. All base-pressure data were therefore corrected to stream conditions without condensation, using the method of reference 12. As pointed out in reference 12, this method probably gives a maximum correction. (See ref. 13 for a more detailed discussion of the effects of condensation on flow about models.) Since there is some uncertainty in this correction, both corrected and uncorrected data are presented for $M_0 = 4.48$ and $M_0 = 4.98$.⁴ As the test airfoils are very slender and produce pressure ratios only slightly above 1, no correction of the surface pressures for air re-evaporation was necessary, as can be seen in figure 11 of reference 13.

The variation in stream Mach number in the region of the airfoil was ± 0.01 or less at all Mach numbers except $M_0 = 4.98$. At this Mach number, the variation in the spanwise direction was ± 0.025 . The variation in stream static pressure was sufficiently small in all cases to make buoyancy corrections negligible. All airfoils were located on the test-section center line, and the variation in stream inclination was disregarded since it was $\pm 0.1^\circ$ or less in all cases. The error in Reynolds number was less than 1 percent.

In general, the force measurements were accurate to within ± 3 percent of the total load on the balance system at the highest Mach number. A small buoyancy correction, due to internal pressure differences in the balance housing, was made to the measured data. No corrections to

⁴Because the local Mach numbers in the region of the base are higher than the free stream, there is also some effect of condensation at $M_0 = 4.03$. However, the correction to the data at this Mach number was within the experimental scatter.

measured forces (exclusive of base force) for condensation and re-evaporation of the air stream at Mach numbers of 4.48 and above were necessary (see previous discussion of surface pressures).

Summarizing, the pressure coefficients are estimated to be accurate to within ± 0.003 , the base pressure ratios to within ± 0.02 , and the drag coefficients to within ± 0.0002 .

RESULTS AND DISCUSSION

Pressure Data

Chordwise pressure distributions.- The pressure coefficients along the midspan of the pressure-distribution model of airfoil 306-T are presented in figure 6.⁵ Comparison is made with the predictions of the relatively simple small-angle, high Mach number approximation to shock-expansion theory (see ref. 8). As shown in reference 8, no significant differences will exist between these predictions and those of exact shock-expansion theory for airfoils like those under consideration. Two sets of theoretical curves are presented. The first set was determined neglecting the distortion of the effective airfoil profile caused by the laminar boundary layer. The second set was obtained including an estimate of this distortion. This estimate was based on the method of reference 14, in which the airfoil profile is changed locally by an amount equal to the displacement thickness of the boundary layer. The displacement thicknesses were calculated using the method of reference 15. Up to a Mach number of 4.48, the increment in pressure coefficient caused by the boundary layer is small except near the leading edge. In this Mach number range, the experimental data agree closely with both sets of theoretical pressure distributions.⁶ At a Mach number of 4.98, the distortion effect of the boundary layer is more pronounced over the entire chord length of the airfoil, and experiment agrees with the theory only after this effect is included. The marked pressure rise near the nose of the airfoil, which results from the rapid build-up of the laminar boundary layer at high Mach numbers and low Reynolds numbers, was also noted for a flat plate in reference 16. The good agreement observed in figure 6 between the experimental results and the theoretical predictions

⁵The test Mach number was sufficiently high in all cases so that the mid-span pressures were not affected by disturbances originating at the airfoil tips.

⁶Some pressure distributions were also calculated with linear and second-order theory. The agreement with linear theory was relatively poor at higher Mach numbers. The agreement with second-order theory was substantially the same as with shock-expansion theory.

gives experimental verification for the conclusion of reference 8, wherein it was observed that the shock-expansion theory has a wide range of applicability at high supersonic speeds. The results given in reference 16 also give additional verification to this conclusion.

Base-pressure survey.- The Reynolds numbers at which the base pressures were measured are presented as a function of Mach number in figure 7. With the exception of $M_0 = 3.49$ and $M_0 = 4.03$, all tests were made at only one Reynolds number for each test Mach number. The Reynolds number ranges for these two Mach numbers are also indicated in figure 7. The base pressures were measured simultaneously with the force data, and no attempt was made to induce artificial transition by adding surface roughness. All results presented are therefore for laminar-boundary-layer flows.

As was stated previously, base-pressure measurements were made at four points on the trailing edge of each airfoil. Typical spanwise distributions of p_b/p_0 for one airfoil, 306-T, are shown in figure 8. Since the spanwise variation is generally small over the test range, the remaining data are presented as arithmetic means of the four individual measurements.

Following the example of reference 9, all base-pressure data are presented in correlated form as a function of the parameter⁷ $c/(h\sqrt{Re})$ (see fig. 9). A small amount of data, not presented in figure 9, was also obtained at $M_0 = 4.67$ and $M_0 = 4.84$. These data show the same trends as those presented. All the data correlate reasonably well to single curves at each Mach number. To show the effects of condensation, uncorrected data for $M_0 = 4.48$ and 4.98 are also shown in figure 9. The design-base-pressure estimates are also shown; those for $M_0 = 3$ are included with the $M_0 = 2.73$ curve. In general, the estimates are within the experimental scatter of the measured data.

To further illustrate the reliability of this method of correlation, the variation of base-pressure ratio with Reynolds number for three different airfoils at a Mach number of 4.03 is shown in figure 10. In correlated form (fig. 9(c)) these data combine reasonably well into segments of the same curve. Some deviations from a single curve are, of course, evident, but these deviations are generally less than the differences in the three distinct curves of figure 10. In general, then, it appears that for airfoils, the methods for correlating base-pressure data that were used at low supersonic speeds in reference 9 are also useful at high supersonic speeds. This result is somewhat in contrast to the results obtained for bodies of revolution in reference 12, where it was observed

⁷As pointed out in reference 9, for laminar boundary layers this parameter is proportional to the ratio of the boundary-layer height at the trailing edge to the base height.

that the corresponding correlation method was not as reliable at high supersonic speeds as at low supersonic speeds.

Force Data

Results of the drag measurements on all the test airfoils are presented in figure 11. The drag coefficients are based on the net forces on the airfoils; that is, they represent the difference between the measured total drag of the wing-body combination and the tare drag of the body.

Comparison of experimental with calculated drag curves is made in figure 11. The calculated drag curves were determined by adding the two-dimensional pressure drag, skin-friction drag, and the measured base drag. The pressure drag was calculated from pressure distributions determined in the same manner as those previously discussed; that is, using the slender-airfoil theory of reference 8 and the distortion effect of the boundary layer after the method of reference 14. The use of section theory to calculate the drag of finite-span airfoils is supported in reference 17, where it is observed that if the aspect ratio is of the order of 1 or greater, flow about wings at high supersonic speeds may be treated as a two-dimensional problem.

In general, the agreement between the calculated and experimental drag coefficients in figure 11 is good. Differences observed at $M_0 = 5.0$ are due in part to the errors in measuring the small forces encountered.⁸ The increase in the total drag coefficients at the high Mach numbers results primarily from the decrease in test Reynolds number as the free-stream Mach number is increased, leading to a corresponding increase in skin-friction drag coefficient.

The drag coefficients of two of the minimum-drag airfoils, 306-T and 506-T, are compared in figure 12 to those of the biconvex airfoil. It is recalled that all three airfoils are designed to have the same torsional rigidity. Consistent with the design conditions of the airfoils, airfoil 306-T has the lowest drag at the lowest Mach numbers, and airfoil 506-T has the lowest drag at the highest Mach numbers. The biconvex airfoil has drag higher than either of the minimum-drag airfoils at their respective design Mach numbers. The largest difference in drag is about 20 percent. It is also apparent from the curves in figure 12 that there is very little difference in drag between the two minimum-drag airfoils at the higher Mach numbers. This result is again attributed mostly to the decrease in pressure-drag coefficient and increase in skin-friction drag coefficient with Mach number at the higher Mach numbers of

⁸It is possible that air condensation, as previously discussed, could also have been a contributing factor, although the pressure data (fig. 6(d)) do not indicate that this is the case.

the present tests. It is evident that because of this effect of skin friction, an airfoil required to operate over the present test range of Mach numbers and Reynolds numbers would have greater drag savings, on the average, if designed for $M_0 = 3$ rather than for $M_0 = 5$. It appears, then, that in some cases it may be worthwhile to consider skin friction in picking the design conditions of an airfoil.

The drag coefficients of two airfoils, 306-B and 506-B, are compared in figure 13. Both these airfoils have the same bending strength. Again, in agreement with the design conditions, airfoil 306-B has the lower drag at the lower Mach numbers and airfoil 506-B has the lower drag at the high Mach numbers. Again, too, the difference in drag is smaller at the high Mach numbers.

The drag coefficients of airfoils 306-T and 306-B are compared in figure 14. Although both airfoils have the same torsional rigidity, only airfoil 306-T was designed for this criterion; airfoil 306-B was designed for a given bending strength. (See Models.) There is very little difference between the drags of the two airfoils; however, at the design Mach number of 3, airfoil 306-T does have slightly lower drag, which is in agreement with theory.

Similar comparisons have been made with the family of four-percent-thick airfoils. The same trends were evident; however, since these airfoils are thinner and have lower drags, the differences in drag coefficients were even less.

CONCLUSIONS

Investigation of the zero-lift-drag characteristics of nine symmetrical airfoils at Mach numbers from 2.7 to 5.0 and Reynolds numbers from 0.35 million to 3.63 million leads to the following conclusions:

1. Pressure distributions can be predicted within engineering accuracy by the use of shock-expansion theory. It is necessary to account for distortion of the effective airfoil profile by the laminar boundary layer at the higher Mach numbers and lower Reynolds numbers of these tests. This result is in agreement with previous experimental and theoretical findings.

2. Base pressures measured on the blunt-trailing-edge airfoils were found to correlate, in the case of laminar boundary layers, against a parameter proportional to the ratio of the boundary-layer thickness at the base to the base height. The correlation curves should prove useful at high supersonic Mach numbers, just as at low supersonic Mach numbers, in estimating design base pressures for blunt-trailing-edge, minimum-pressure-drag airfoils.

3. Each minimum-drag airfoil had, at its particular design conditions, the lowest drag of all comparable airfoils tested. The largest saving in drag was about 20 percent. The differences in drag at higher Mach numbers were quite small, due in good part to a decrease in pressure drag relative to skin-friction drag. The results showed that because of this effect of skin friction, an airfoil required to operate over the present test range of Mach numbers and Reynolds numbers would have greater drag savings, on the average, if designed for a Mach number of 3 rather than for a Mach number of 5. It appears, then, that in some cases it may be worthwhile to consider skin friction in picking the design conditions of an airfoil.

Ames Aeronautical Laboratory
National Advisory Committee for Aeronautics
Moffett Field, Calif.

REFERENCES

1. Drougge, Georg: Wing Sections with Minimum Drag at Supersonic Speeds. Rep. No. 26, Aero. Res. Inst. of Sweden (Stockholm) 1949.
2. Chapman, Dean R.: Reduction of Profile Drag at Supersonic Velocities by the Use of Airfoil Sections Having a Blunt Trailing Edge. NACA RM A9H11, 1949.
3. Chapman, Dean R.: Airfoil Profiles for Minimum Pressure Drag at Supersonic Velocities - General Analysis with Application to Linearized Supersonic Flow. NACA Rep. 1063, 1952. (Formerly NACA TN 2264).
4. Klunker, E. B., and Harder, Keith C.: Comparison of Supersonic Minimum-Drag Airfoils Determined by Linear and Nonlinear Theory. NACA TN 2623, 1952.
5. Ivey, H. Reese, and Cline, Charles W.: Effect of Heat-Capacity Lag on the Flow Through Oblique Shock Waves. NACA TN 2196, 1950.
6. Chapman, Dean R.: Airfoil Profiles for Minimum Pressure Drag at Supersonic Velocities - Application of Shock-Expansion Theory, Including Consideration of Hypersonic Range. NACA TN 2787, 1952.
7. Epstein, Paul S.: On the Air Resistance of Projectiles. Proceedings of the National Academy of Sciences, vol. 17, 1931, pp. 532-547.

8. Eggers, A. J., Jr., and Syvertson, Clarence A.: Inviscid Flow About Airfoils at High Supersonic Speeds. NACA TN 2646, 1952.
9. Chapman, Dean R., Wimbrow, William R., and Kester, Robert H.: Experimental Investigation of Base Pressure on Blunt-Trailing-Edge Wings at Supersonic Velocities. NACA TN 2611, 1952.
10. Eggers, A. J., Jr., Dennis, David H., and Resnikoff, Meyer M.: Bodies of Revolution for Minimum Drag at High Supersonic Airspeeds. NACA RM A51K27, 1952.
11. Katzen, Elliott D., and Kaattari, George E.: Drag Interference Between a Pointed Cylindrical Body and Triangular Wings of Various Aspect Ratios at Mach Numbers of 1.50 and 2.02. NACA RM A51C27, 1951.
12. Reller, John O., Jr., and Hamaker, Frank M.: An Experimental Investigation of the Base Pressure Characteristics of Nonlifting Bodies of Revolution at Mach Numbers From 2.73 to 4.98. NACA RM A52E20, 1952.
13. Hansen, C. Frederick, and Nothwang, George J.: Condensation of Air in Supersonic Wind Tunnels and Its Effects on Flow About Models. NACA TN 2690, 1952.
14. Bertram, Mitchel H.: An Approximate Method for Determining the Displacement Effects and Viscous Drag of Laminar Boundary Layers in Two-Dimensional Hypersonic Flow. NACA TN 2773, 1952.
15. Young, A. D.: Skin Friction in the Laminar Boundary Layer in Compressible Flow. The Aeronautical Quarterly, vol. I, part II, Aug. 1949, pp. 137-164.
16. McLellan, Charles H., Bertram, Mitchell H., and Moore, John A.: An Investigation of Four Wings of Square Plan Form at a Mach Number of 6.86 in the Langley 11-Inch Hypersonic Tunnel. NACA RM L51D17, 1951.
17. Hamaker, Frank M., Neice, Stanford E., and Eggers, A. J., Jr.: The Similarity Law for Hypersonic Flow About Slender Three-Dimensional Shapes. NACA TN 2443, 1951.

TABLE I.- AIRFOIL DESIGN CONDITIONS AND STRUCTURAL PROPERTIES

| Airfoil | Design Mach number | t/c | h/c | h/t | Moment of inertia about chord axis, in. ⁴ | Section modulus, in. ³ |
|----------|-----------------------|--------|--------|-------|---|---|
| 304-T | 3 | 0.0400 | 0.0226 | 0.564 | 41.6×10^{-6} | 10.4×10^{-4} |
| 504-T | 5 | .0399 | .0348 | .871 | 41.6×10^{-6} | 10.4×10^{-4} |
| 304-B | 3 | .0376 | .0233 | .621 | 41.6×10^{-6} | 11.0×10^{-4} |
| 504-B | 5 | .0374 | .0336 | .898 | 41.2×10^{-6} | 11.0×10^{-4} |
| 306-T | 3 | .0600 | .0356 | .594 | 138.7×10^{-6} | 23.1×10^{-4} |
| 506-T | 5 | .0598 | .0528 | .884 | 138.7×10^{-6} | 23.2×10^{-4} |
| 306-B | 3 | .0562 | .0376 | .669 | 138.7×10^{-6} | 24.8×10^{-4} |
| 506-B | 5 | .0563 | .0513 | .912 | 139.4×10^{-6} | 24.8×10^{-4} |
| Biconvex | - | .0610 | 0 | 0 | 138.7×10^{-6} | 22.7×10^{-4} |

Key to airfoil identification:

Airfoil 3 06 - T

Design structural condition
(T Torsional rigidity)
(B Bending strength)

Approximate t/c

Design Mach number



~~CONFIDENTIAL~~

TABLE II.- AIRFOIL COORDINATES IN INCHES

| Airfoil 304-T | | Airfoil 504-T | |
|---------------|--------------------|---------------|--------------------|
| Abscissa x | Ordinate y | Abscissa x | Ordinate y |
| 0 | 0 | 0 | 0 |
| .100 | .0042 | .100 | .0034 |
| .200 | .0084 | .200 | .0069 |
| .300 | .0126 | .300 | .0103 |
| .400 | .0168 | .400 | .0137 |
| .500 | .0209 | .500 | .0172 |
| .600 | .0248 | .600 | .0205 |
| .700 | .0283 | .700 | .0237 |
| .800 | .0315 | .800 | .0267 |
| .900 | .0343 | .900 | .0294 |
| 1.000 | .0367 | 1.000 | .0320 |
| 1.100 | .0384 | 1.100 | .0343 |
| 1.200 | .0395 | 1.200 | .0363 |
| 1.300 | .0400 ^a | 1.300 | .0379 |
| 1.400 | .0395 | 1.400 | .0391 |
| 1.500 | .0382 | 1.500 | .0397 |
| 1.600 | .0360 | 1.573 | .0399 ^a |
| 1.700 | .0333 | 1.600 | .0399 |
| 1.800 | .0301 | 1.700 | .0394 |
| 1.900 | .0264 | 1.800 | .0383 |
| 2.000 | .0226 | 1.900 | .0368 |
| - - - | - - - | 2.000 | .0348 |
| Airfoil 304-B | | Airfoil 504-B | |
| Abscissa x | Ordinate y | Abscissa x | Ordinate y |
| 0 | 0 | 0 | 0 |
| .100 | .0047 | .100 | .0039 |
| .200 | .0094 | .200 | .0078 |
| .300 | .0142 | .300 | .0116 |
| .400 | .0189 | .400 | .0155 |
| .500 | .0234 | .500 | .0194 |
| .600 | .0273 | .600 | .0230 |
| .700 | .0307 | .700 | .0264 |
| .800 | .0336 | .800 | .0294 |
| .900 | .0357 | .900 | .0321 |
| 1.000 | .0372 | 1.000 | .0343 |
| 1.087 | .0376 ^a | 1.100 | .0361 |
| 1.477 | .0376 ^a | 1.200 | .0371 |
| 1.500 | .0376 | 1.295 | .0374 ^a |
| 1.600 | .0368 | 1.689 | .0374 ^a |
| 1.700 | .0350 | 1.700 | .0374 |
| 1.800 | .0322 | 1.800 | .0368 |
| 1.900 | .0283 | 1.900 | .0356 |
| 2.000 | .0233 | 2.000 | .0336 |

^a maximum ordinates~~CONFIDENTIAL~~

TABLE II.- AIRFOIL COORDINATES IN INCHES - Concluded

| Airfoil 306-T | | Airfoil 506-T | | Biconvex airfoil | |
|---------------|--------------------|---------------|--------------------|------------------|--------------------|
| Abscissa x | Ordinate y | Abscissa x | Ordinate y | Abscissa x | Ordinate y |
| 0 | 0 | 0 | 0 | 0 | 0 |
| .100 | .0061 | .100 | .0050 | .100 | .0116 |
| .200 | .0122 | .200 | .0099 | .200 | .0220 |
| .300 | .0183 | .300 | .0149 | .300 | .0311 |
| .400 | .0244 | .400 | .0199 | .400 | .0391 |
| .500 | .0302 | .500 | .0248 | .500 | .0458 |
| .600 | .0357 | .600 | .0296 | .600 | .0513 |
| .700 | .0411 | .700 | .0343 | .700 | .0556 |
| .800 | .0459 | .800 | .0389 | .800 | .0586 |
| .900 | .0502 | .900 | .0431 | .900 | .0604 |
| 1.000 | .0539 | 1.000 | .0470 | 1.000 | .0610 ^a |
| 1.100 | .0569 | 1.100 | .0504 | 1.100 | .0604 |
| 1.200 | .0588 | 1.200 | .0533 | 1.200 | .0586 |
| 1.300 | .0598 | 1.300 | .0558 | 1.300 | .0556 |
| 1.342 | .0600 ^a | 1.400 | .0578 | 1.400 | .0513 |
| 1.400 | .0598 | 1.500 | .0592 | 1.500 | .0458 |
| 1.500 | .0582 | 1.600 | .0598 | 1.600 | .0391 |
| 1.600 | .0555 | 1.613 | .0598 ^a | 1.700 | .0311 |
| 1.700 | .0521 | 1.700 | .0594 | 1.800 | .0220 |
| 1.800 | .0477 | 1.800 | .0581 | 1.900 | .0116 |
| 1.900 | .0423 | 1.900 | .0560 | 2.000 | 0 |
| 2.000 | .0356 | 2.000 | .0529 | - - - | - - - |

| Airfoil 306-B | | Airfoil 506-B | |
|---------------|--------------------|---------------|--------------------|
| Abscissa x | Ordinate y | Abscissa x | Ordinate y |
| 0 | 0 | 0 | 0 |
| .100 | .0068 | .100 | .0056 |
| .200 | .0136 | .200 | .0113 |
| .300 | .0203 | .300 | .0169 |
| .400 | .0271 | .400 | .0225 |
| .500 | .0334 | .500 | .0280 |
| .600 | .0393 | .600 | .0333 |
| .700 | .0445 | .700 | .0383 |
| .800 | .0489 | .800 | .0430 |
| .900 | .0526 | .900 | .0471 |
| 1.000 | .0549 | 1.000 | .0507 |
| 1.100 | .0561 | 1.100 | .0534 |
| 1.125 | .0562 ^a | 1.200 | .0552 |
| 1.517 | .0562 ^a | 1.300 | .0562 |
| 1.600 | .0554 | 1.334 | .0563 ^a |
| 1.700 | .0532 | 1.720 | .0563 ^a |
| 1.800 | .0495 | 1.800 | .0559 |
| 1.900 | .0444 | 1.900 | .0541 |
| 2.000 | .0376 | 2.000 | .0514 |

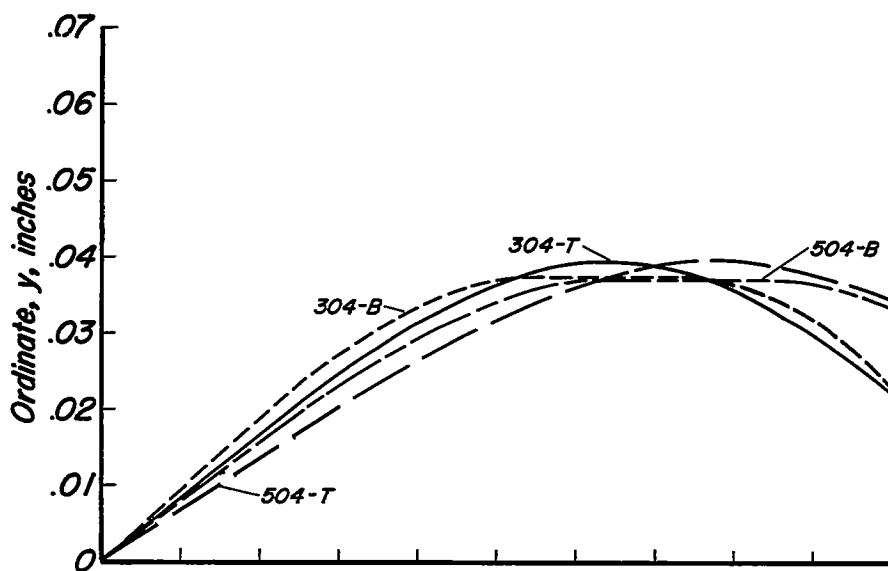
^amaximum ordinates

NACA

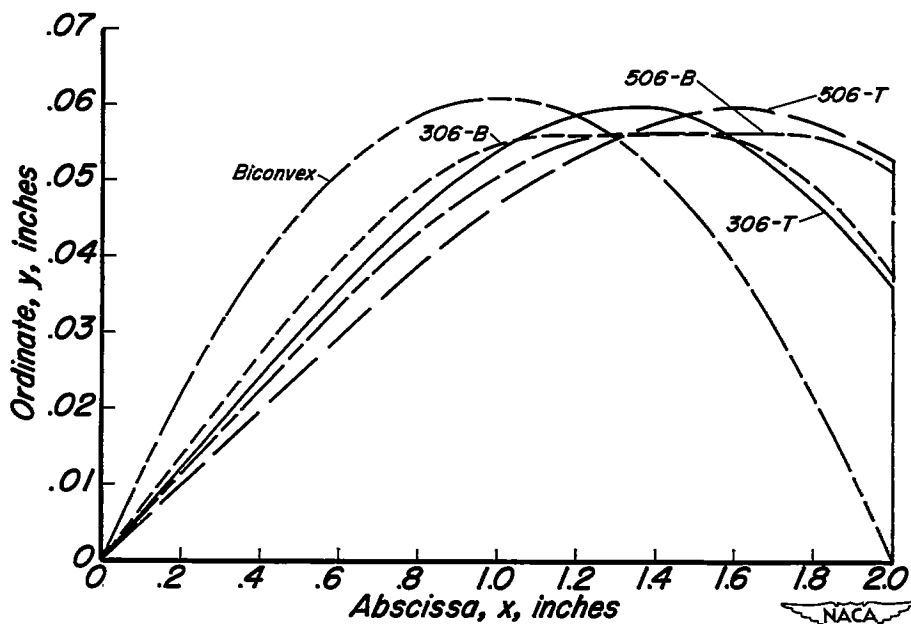
~~CONFIDENTIAL~~

NACA RM A53B02

~~CONFIDENTIAL~~



(a) Airfoils approximately 4 percent thick.



(b) Airfoils approximately 6 percent thick.

Figure 1.- Sketch of the airfoil profiles with expanded vertical scale.

~~CONFIDENTIAL~~

NACA RM A53B02

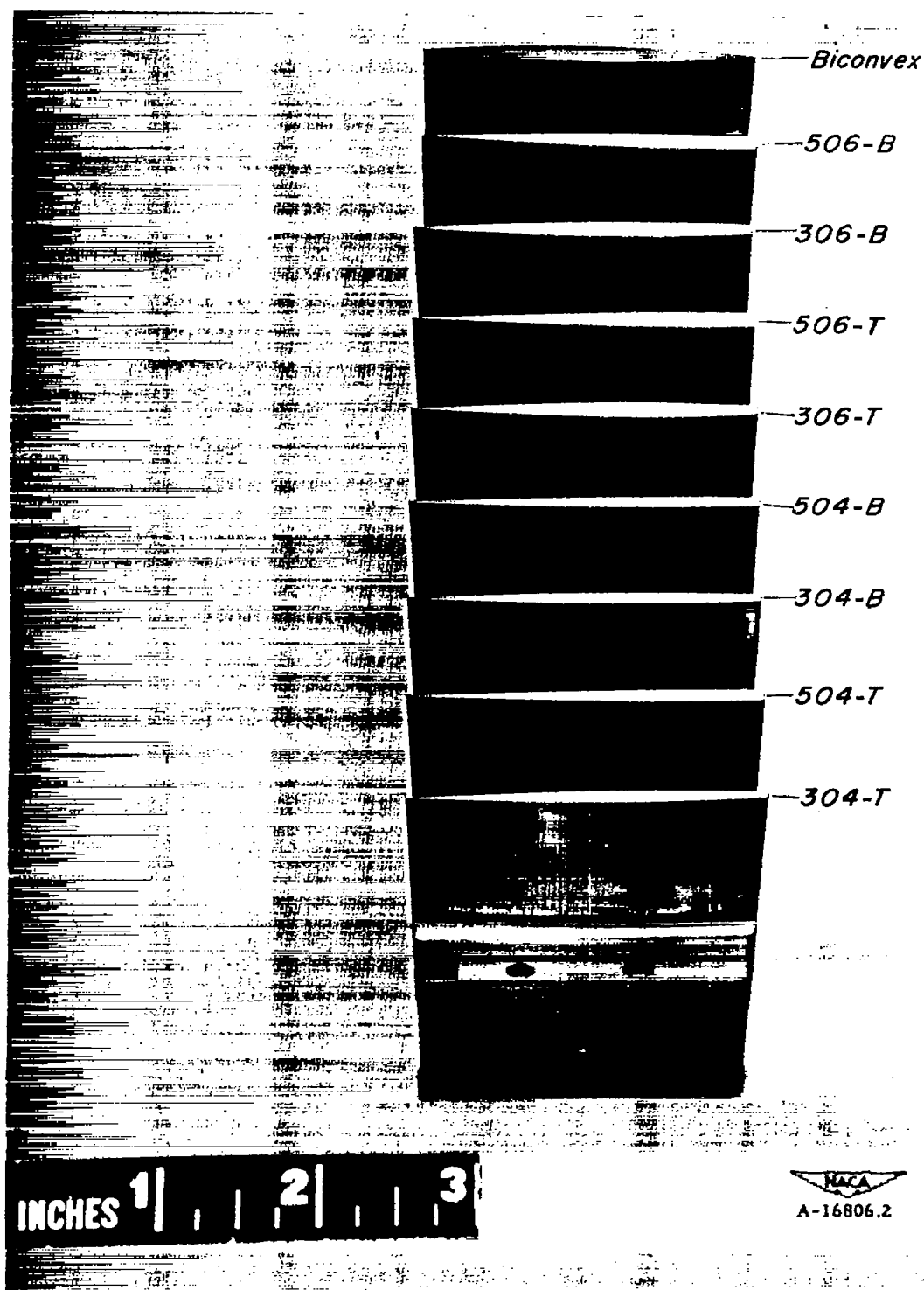
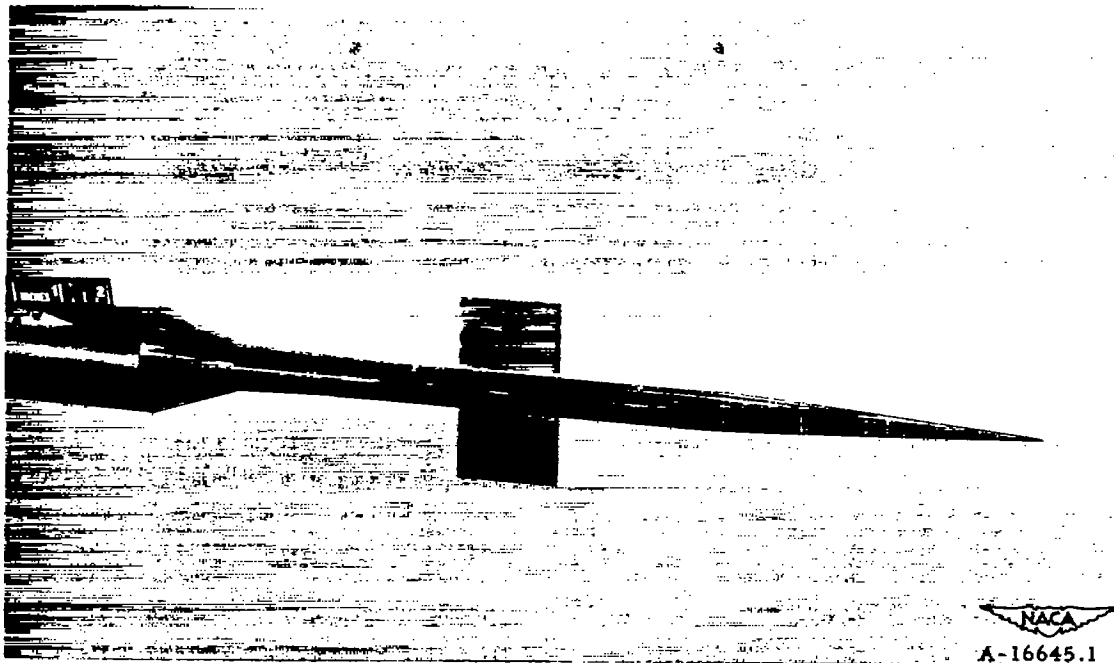
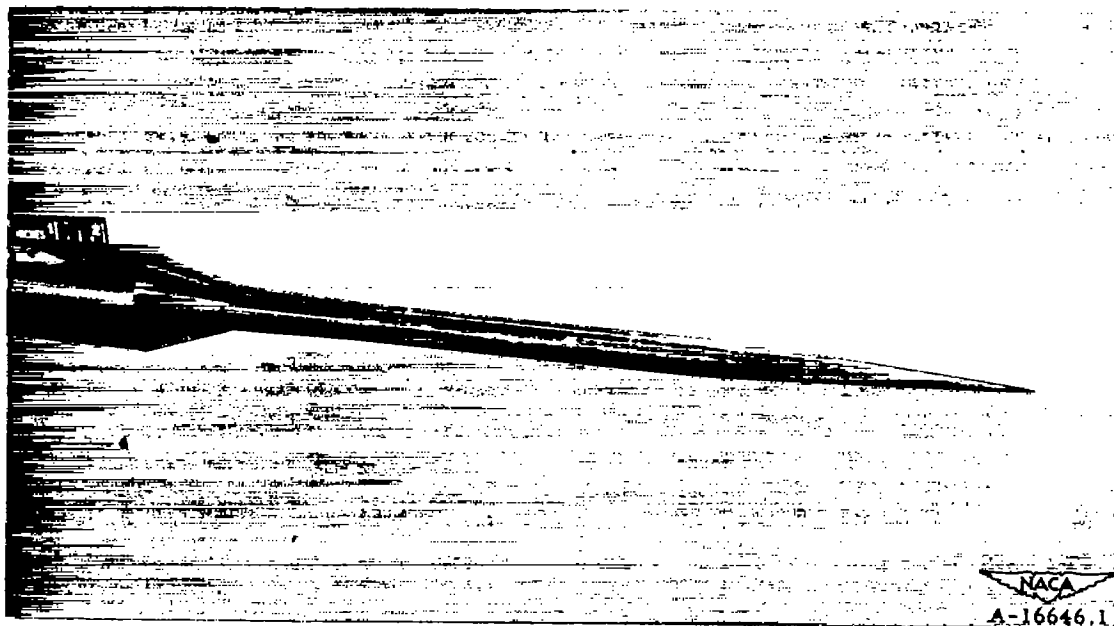


Figure 2.- Force models.

~~CONFIDENTIAL~~



(a) Wing mounted in position.



(b) Support body alone.

Figure 3.- Force model test installation.

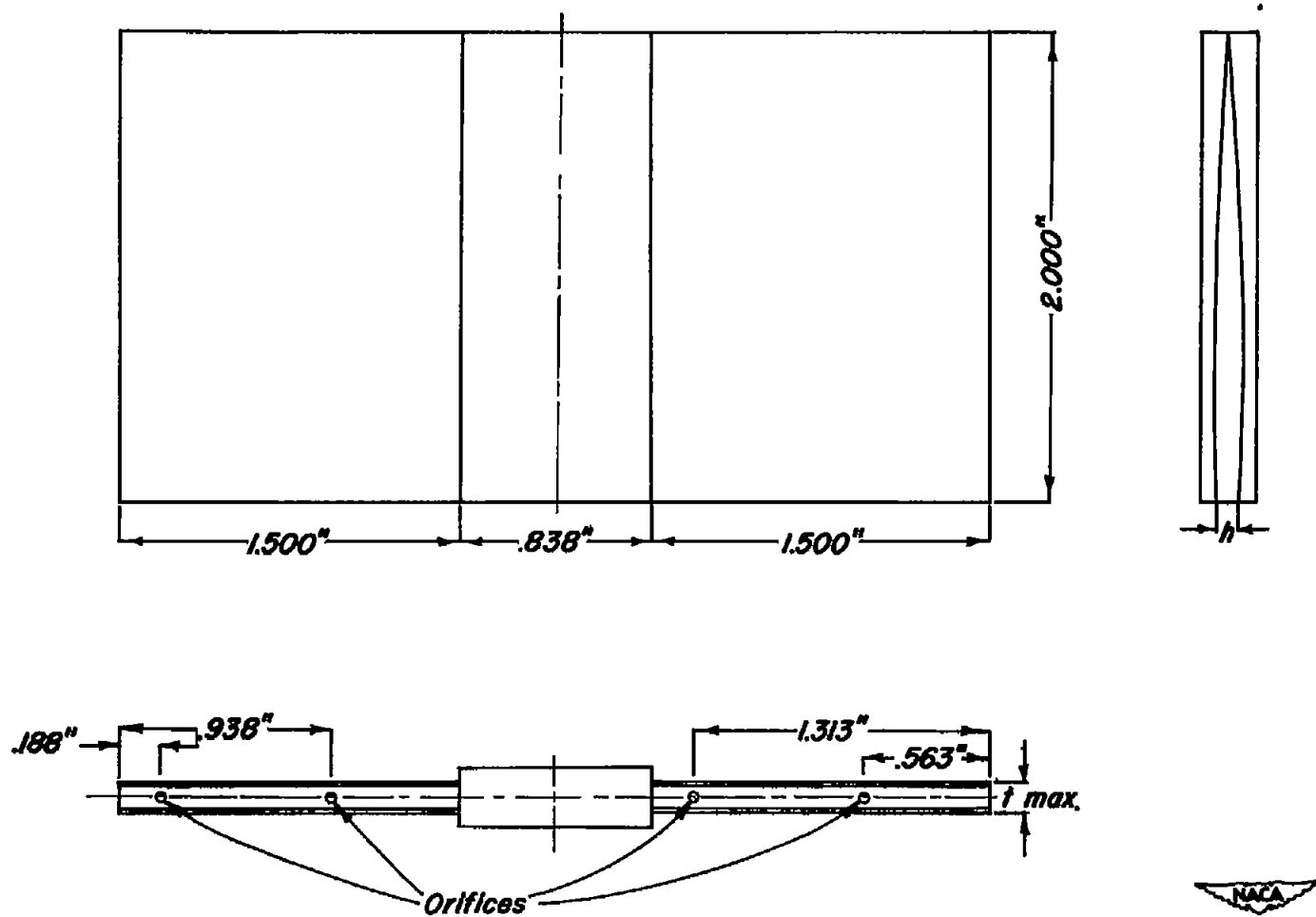


Figure 4.- Sketch of typical blunt-trailing-edge airfoil showing base-pressure orifice locations.

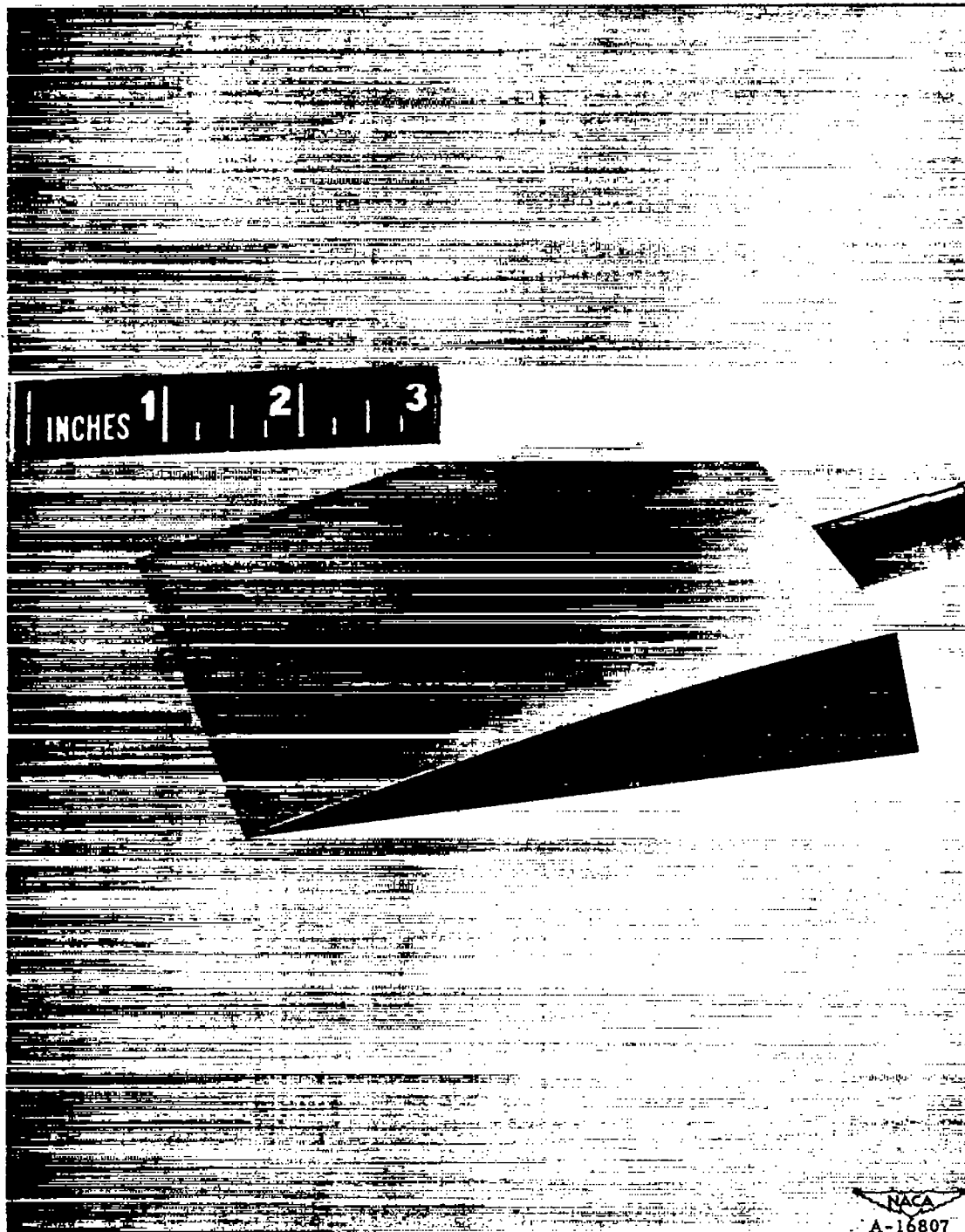


Figure 5.- Pressure-distribution model of airfoil 306-T.

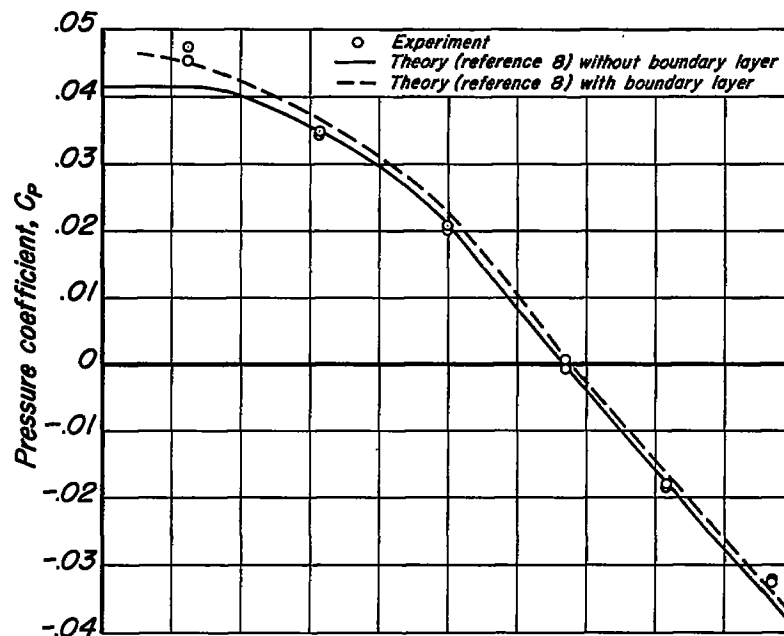
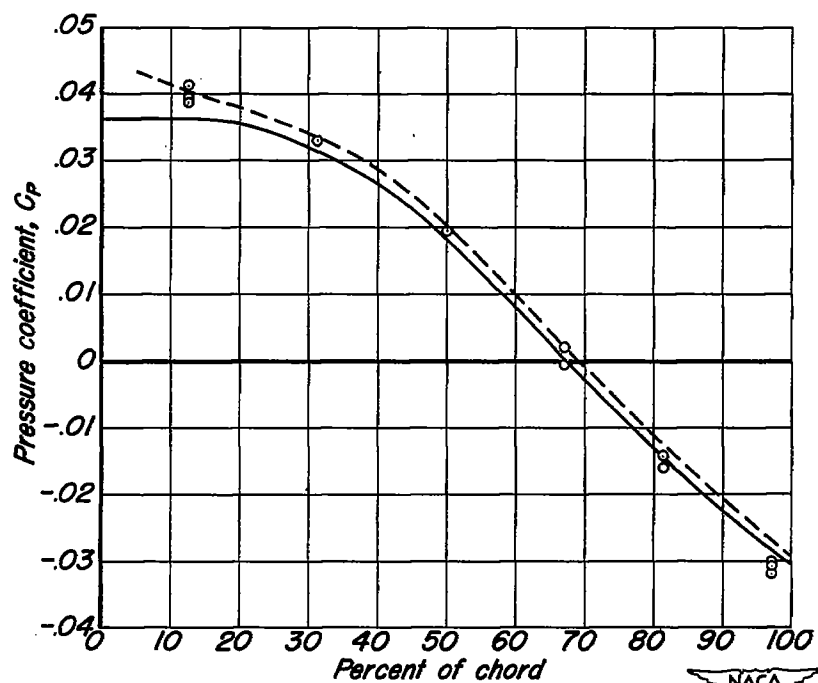
(a) $M_o = 3.49$, $Re = 3.63 \times 10^6$ (b) $M_o = 4.03$, $Re = 2.88 \times 10^6$

Figure 6.-The pressure distribution on airfoil 306-T for several free-stream Mach numbers.

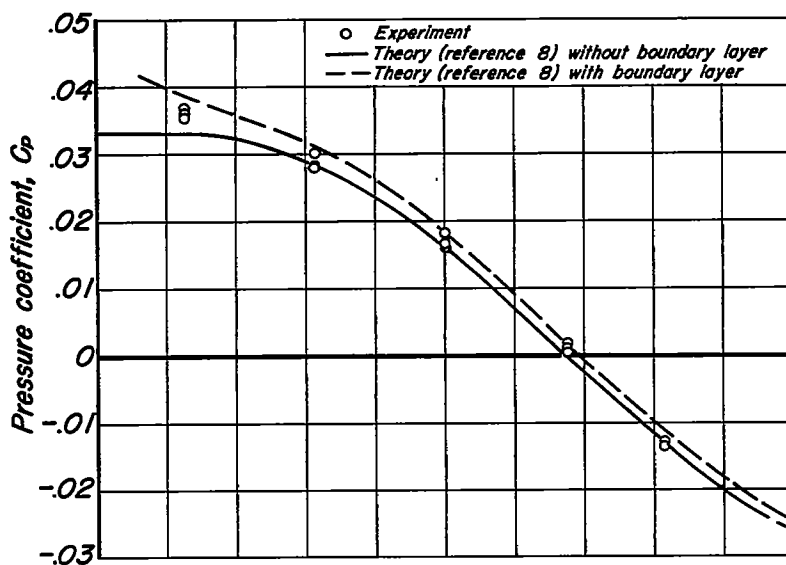
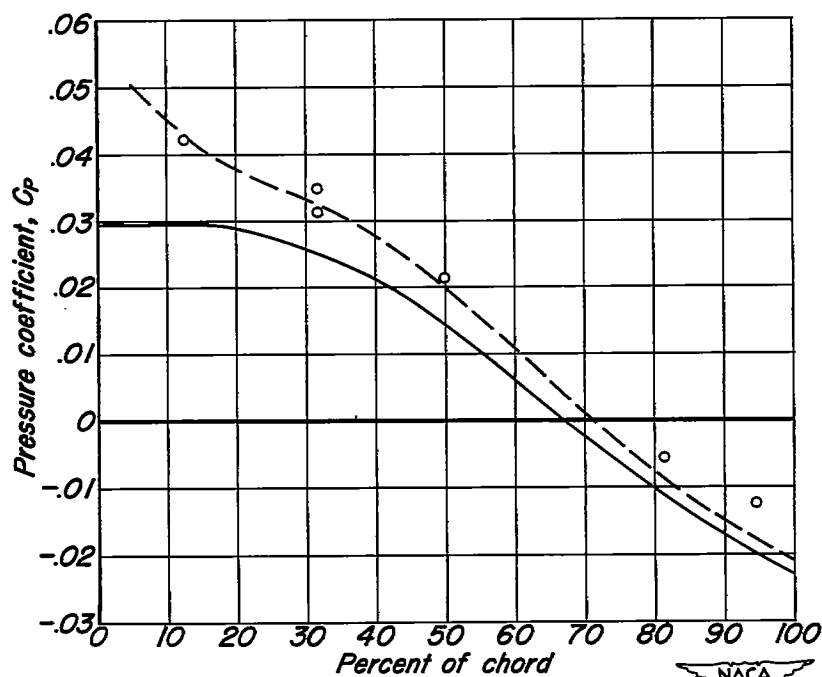
(c) $M_o = 4.48$, $Re = 2.22 \times 10^6$ (d) $M_o = 4.98$, $Re = 0.717 \times 10^6$

Figure 6.-Concluded.

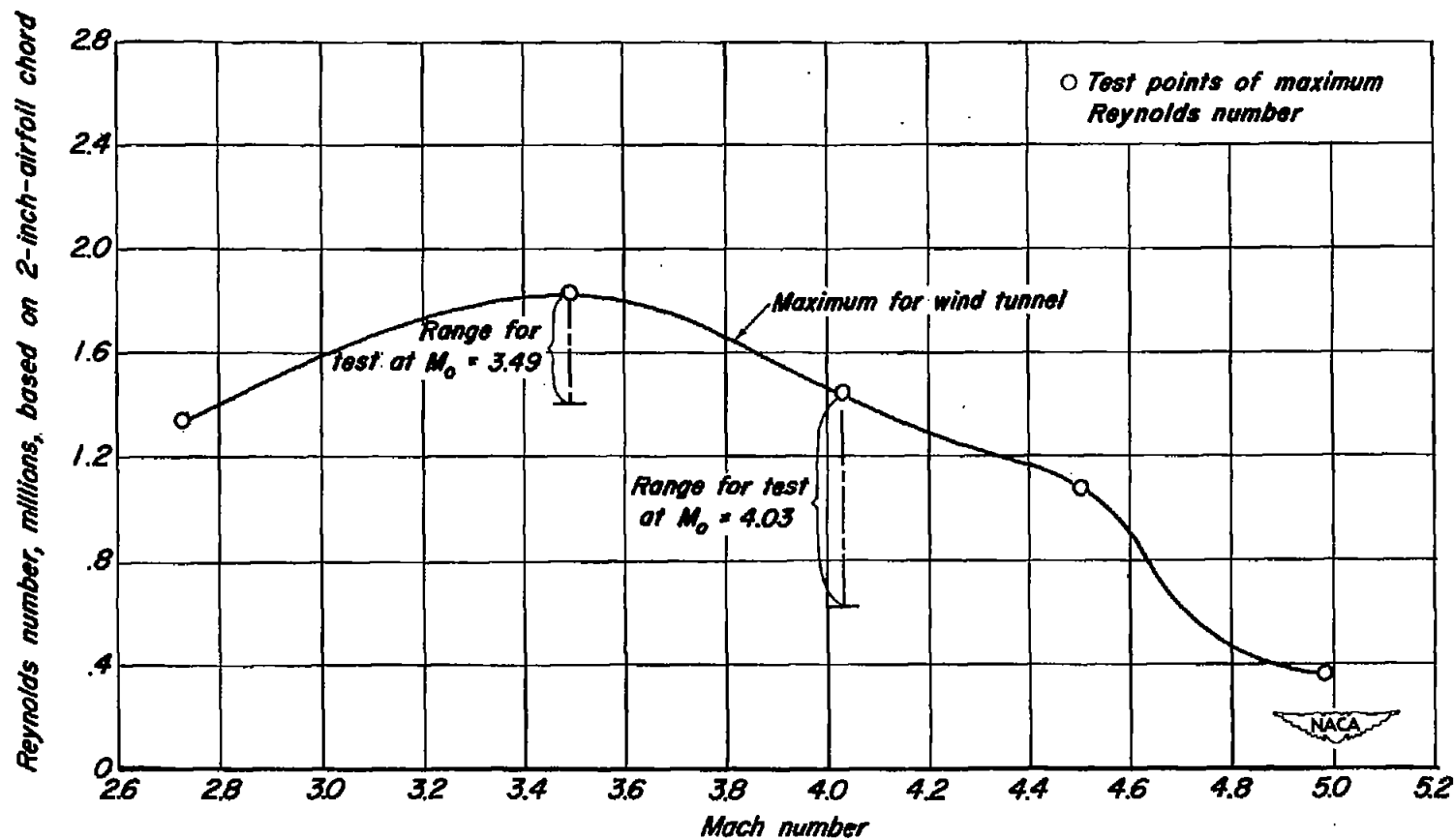


Figure 7.-Variation of Reynolds number with Mach number.

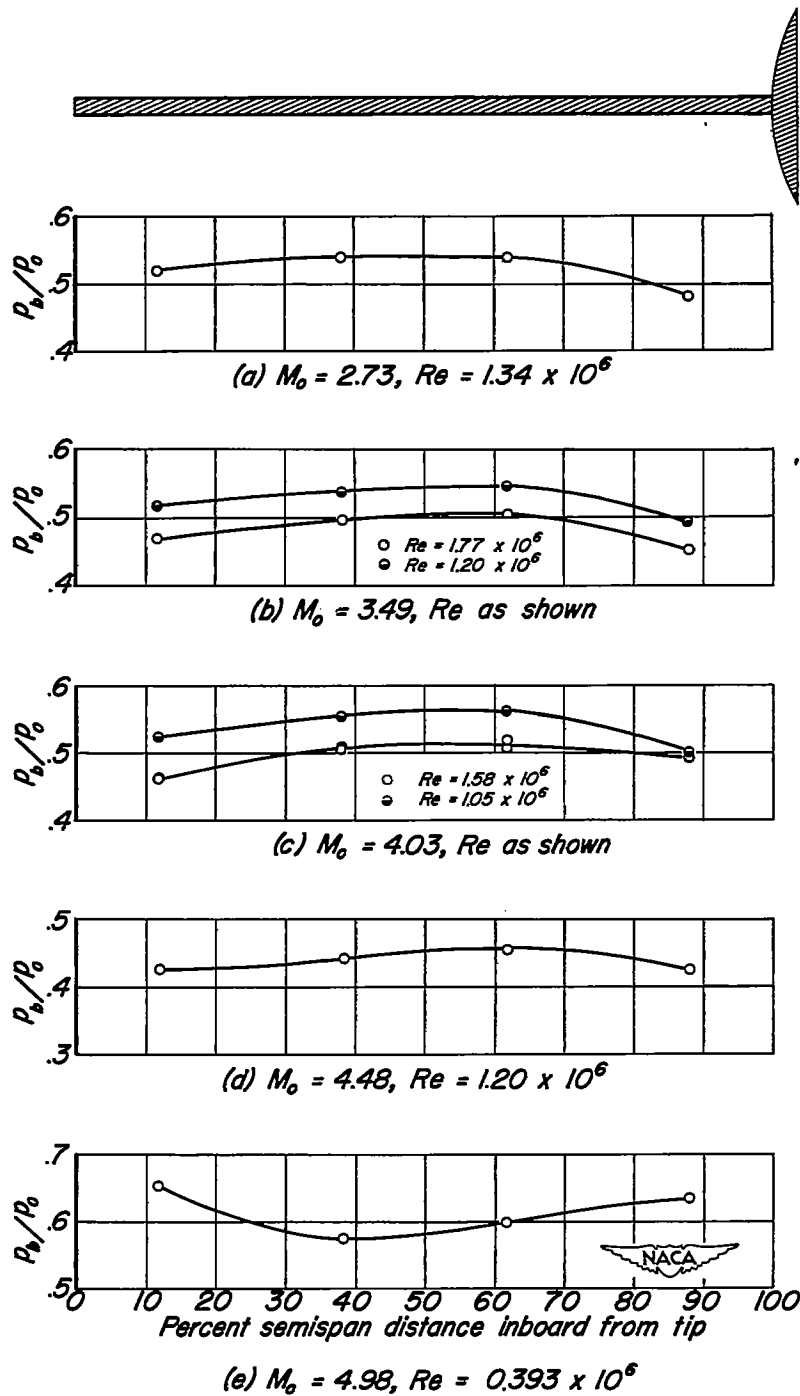


Figure 8.- Typical spanwise base-pressure distribution for airfoil 306-T with laminar boundary layer.

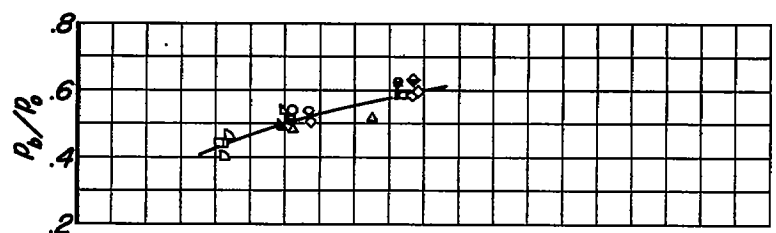
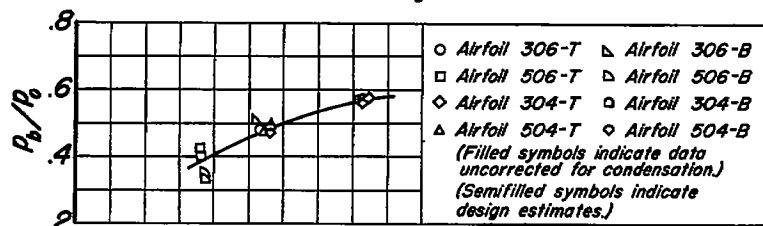
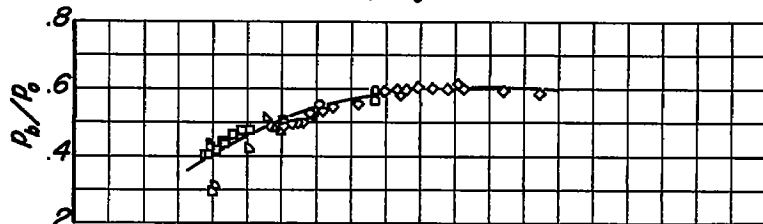
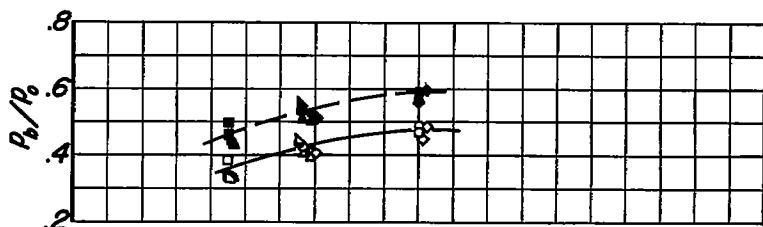
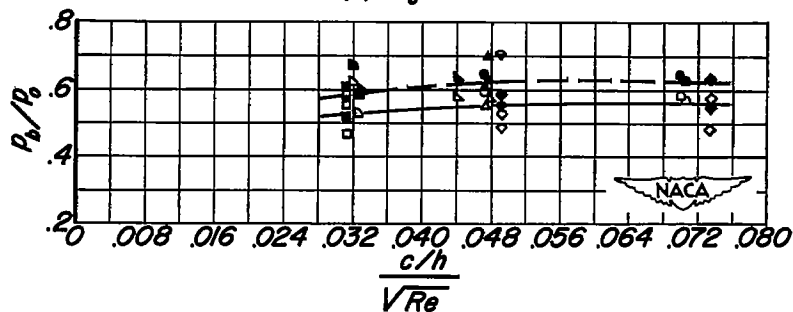
(a) $M_o = 2.73$ (b) $M_o = 3.49$ (c) $M_o = 4.03$ (d) $M_o = 4.48$ (e) $M_o = 4.98$

Figure 9.—Correlated base-pressure data.

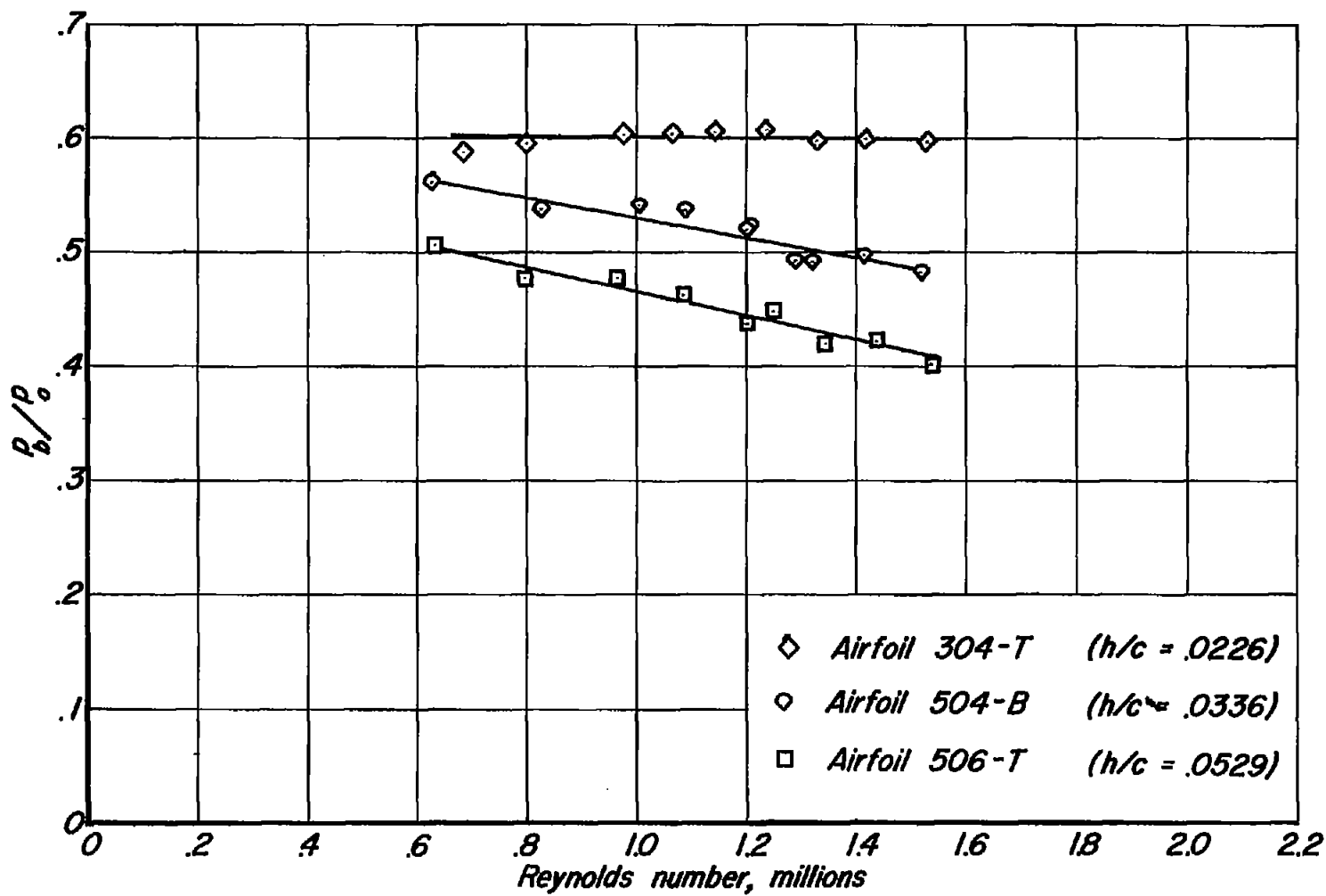
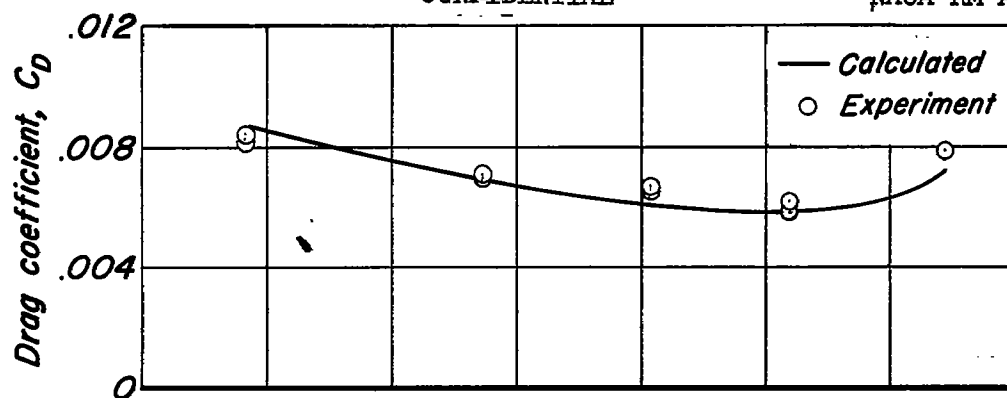


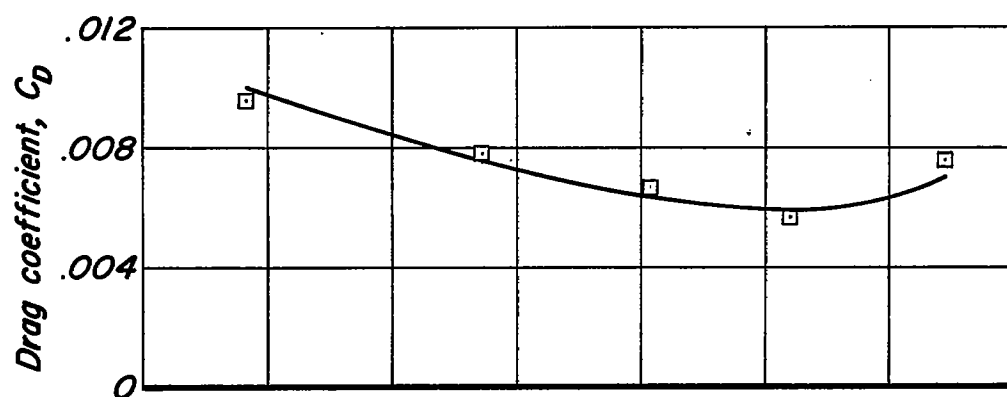
Figure 10.—Variation of base-pressure ratio with Reynolds number at $M_0 = 4.03$.

~~CONFIDENTIAL~~

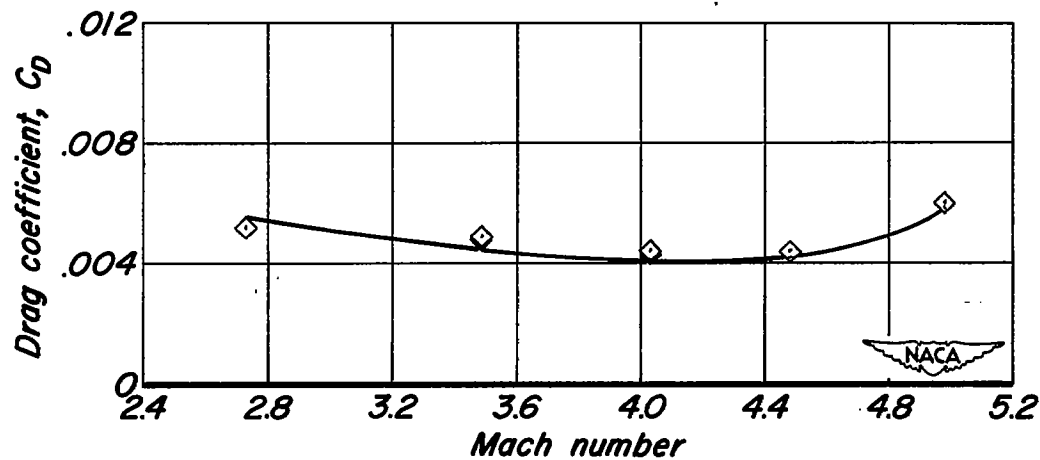
NACA RM A53B02



(a) Airfoil 306-T



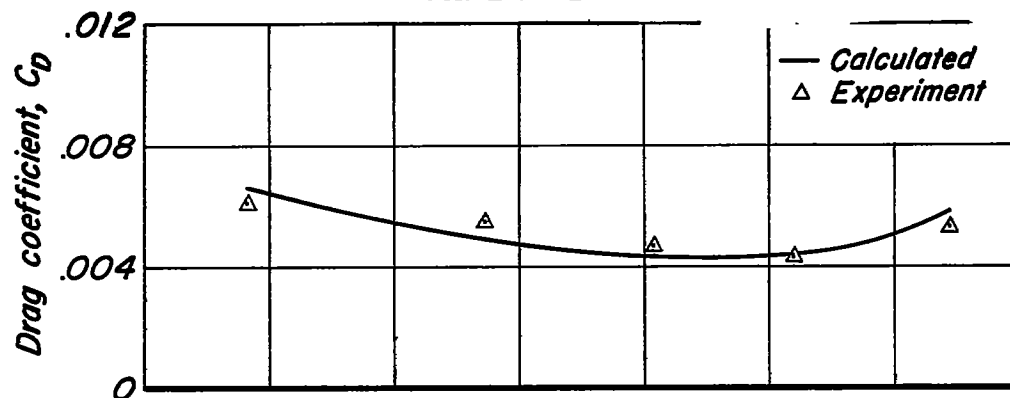
(b) Airfoil 506-T



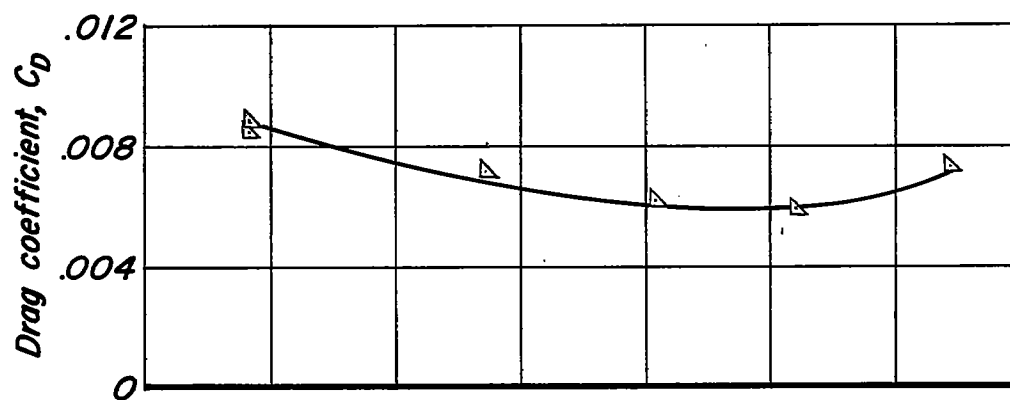
(c) Airfoil 304-T

Figure 11.— Variation of drag coefficient with Mach number.

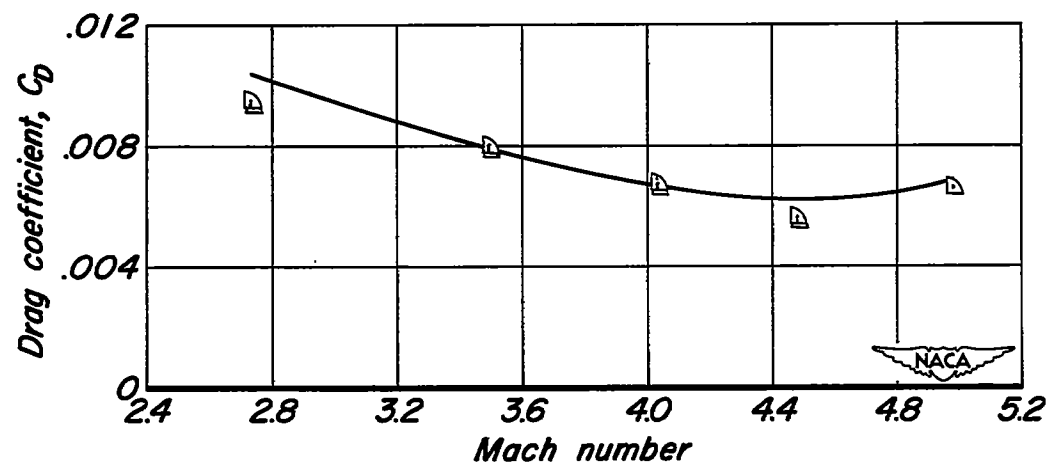
~~CONFIDENTIAL~~



(d) Airfoil 504-T

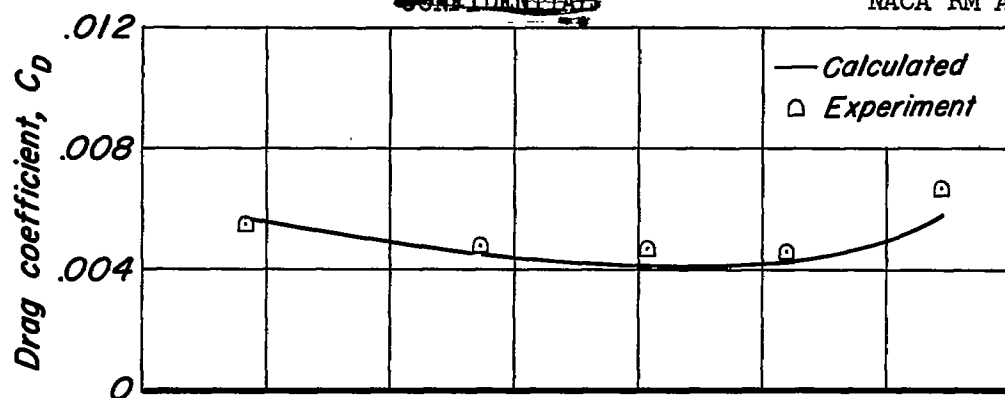


(e) Airfoil 306-B

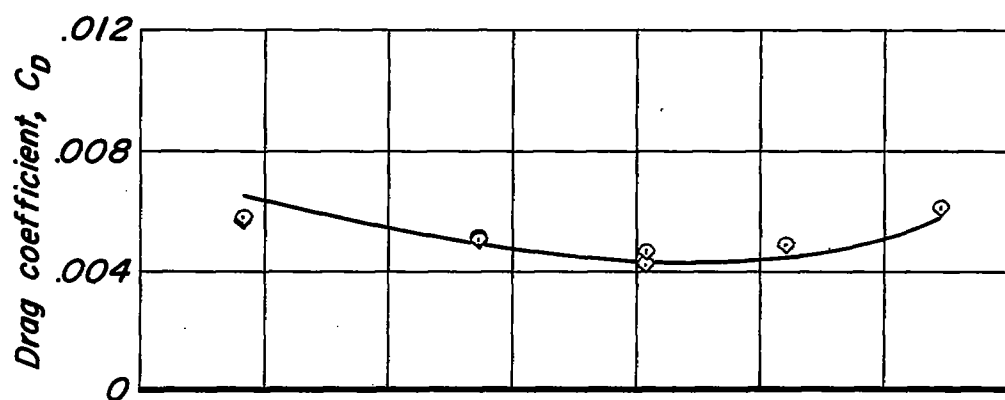


(f) Airfoil 506-B

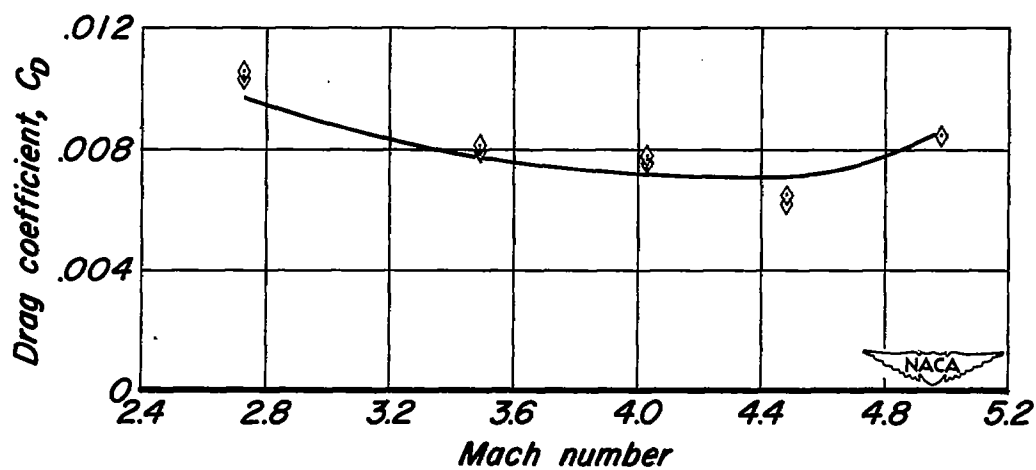
Figure 11.— Continued.

~~CONFIDENTIAL~~

(g) Airfoil 304-B



(h) Airfoil 504-B



(i) Biconvex airfoil

Figure 11.- Concluded.

~~CONFIDENTIAL~~

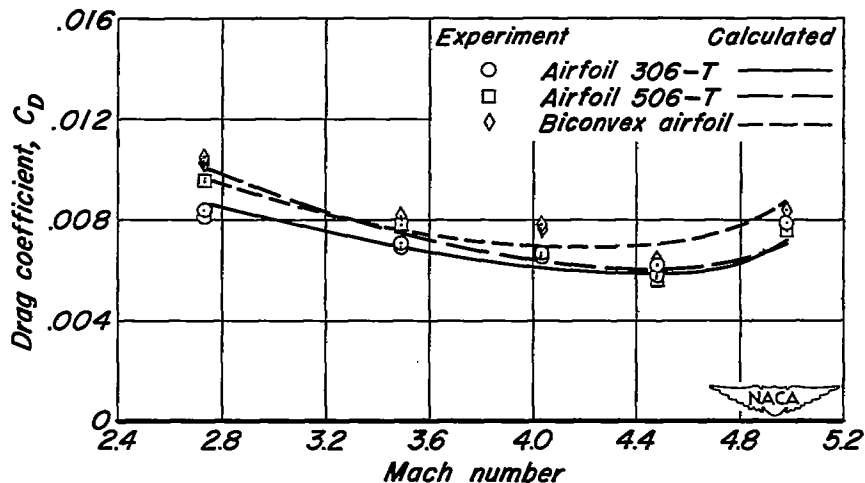


Figure 12.— Variation of drag coefficient with Mach number for airfoils 306-T, 506-T, and biconvex.

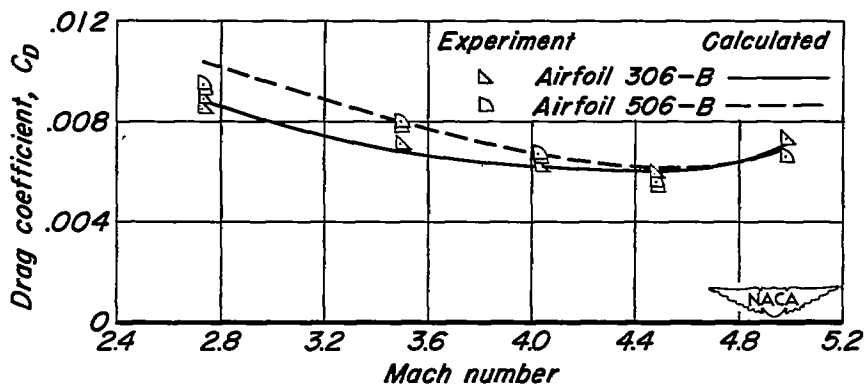


Figure 13.— Variation of drag coefficient with Mach number for airfoils 306-B and 506-B.

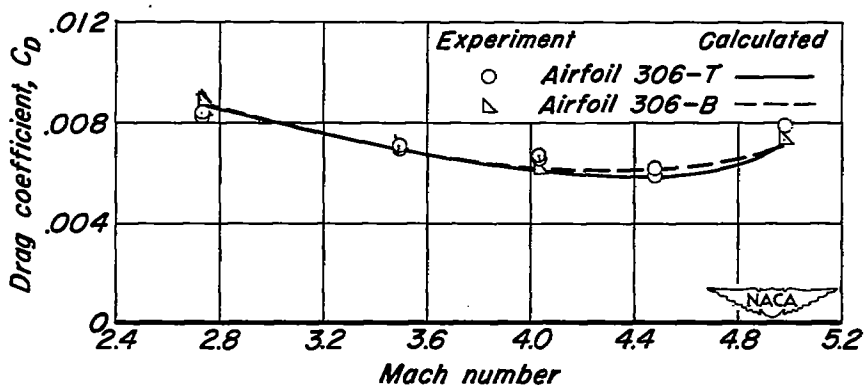


Figure 14.— Variation of drag coefficient with Mach number for airfoils 306-T and 306-B.

~~CONFIDENTIAL~~